INFECTION AND IMMUNITY, July 2010, p. 2946–2955 Vol. 78, No. 7
0019-9567/10/$12.00 doi:10.1128/IAI.01296-09

Milestones in Progression of Primary Pneumonic Plague in Cynomolgus Macaques▽

Frederick Koster,[1]* David S. Perlin,[2] Steven Park,[2] Trevor Brasel,[1] Andrew Gigliotti,[1] Edward Barr,[1] Leslie Myers,[1] Robert C. Layton,[1] Robert Sherwood,[1] and C. R. Lyons[3]

Lovelace Respiratory Research Institute, Albuquerque, New Mexico[1]; Public Health Research Institute at the International Center for Public Health, NJMS-UMDNJ, Newark, New Jersey[2]; and Departments of Pathology and Internal Medicine, University of New Mexico Health Science Center, Albuquerque, New Mexico[3]

Received 19 November 2009/Returned for modification 30 December 2009/Accepted 5 April 2010

Vaccines against primary pneumonic plague, a potential bioweapon, must be tested for efficacy in well-characterized nonhuman primate models. Telemetered cynomolgus macaques (*Macaca fascicularis*) were challenged by the aerosol route with doses equivalent to approximately 100 50% effective doses of *Yersinia pestis* strain CO92 and necropsied at 24-h intervals postexposure (p.e.). Data for telemetered heart rates, respiratory rates, and increases in the temperature greater than the diurnal baseline values identified the onset of the systemic response at 55 to 60 h p.e. in all animals observed for at least 70 h p.e. Bacteremia was detected at 72 h p.e. by a *Yersinia* 16S rRNA-specific quantitative reverse transcription-PCR and was detected later by the culture method at the time of moribund necropsy. By 72 h p.e. multilobar pneumonia with diffuse septal inflammation consistent with early bacteremia was established, and all lung tissues had a high bacterial burden. The levels of cytokines or chemokines in serum were not significantly elevated at any time, and only the interleukin-1β, CCL2, and CCL3 levels were elevated in lung tissue. Inhalational plague in the cynomolgus macaque inoculated by the aerosol route produces most clinical features of the human disease, and in addition the disease progression mimics the disease progression from the anti-inflammatory phase to the proinflammatory phase described for the murine model. Defined milestones of disease progression, particularly the onset of fever, tachypnea, and bacteremia, should be useful for evaluating the efficacy of candidate vaccines.

Primary pneumonic plague is rarely acquired under natural conditions (5, 9, 22), but the virulence and ease of aerosolization make *Yersinia pestis* a potential aerosolized bioweapon (13). The FDA "animal rule" allows the use of large animal models to substitute for human testing if the disease in the model mimics human disease and is well characterized (11). Adequate characterization should include the cause of death, phases of disease progression, and definition of secondary endpoints of success in addition to the primary endpoint of a reduction in mortality.

Primary pneumonic plague in the murine model following intranasal inoculation has been described well (3, 14, 20). The murine model mimics the human infection with respect to high mortality, focal consolidation in the lung, and high levels of bacteremia and dissemination to the liver and the spleen. The murine infection is described as a two-phase disease with an initial anti-inflammatory phase lasting 36 to 48 h after intranasal inoculation, followed by a rapidly progressing proinflammatory phase until death occurs at 4 days postinfection (3, 14).

Nonhuman primates (NHP) are susceptible to aerosolized *Y. pestis*, which produces a rapidly fatal disease similar to that seen in humans with primary pneumonic plague. Different species of NHP may display different susceptibilities and disease progressions after exposure to *Y. pestis* in an aerosol form (7, 8, 10, 16), and a workshop has recommended thorough characterization of the disease in multiple species (11). An initial report described the 50% effective dose (ED_{50}) for aerosolized *Y. pestis* strain CO92 in cynomolgus macaques (21), and this study expanded this model to examine in more detail the progression of disease in telemetered macaques.

MATERIALS AND METHODS

Animals. Both male and female cynomolgus macaques (*Macaca fasicularis*) of Indonesian origin were supplied by Covance, and they weighed 2.5 to 3.5 kg. These animals were screened for the presence of B-virus, simian immunodeficiency virus (SIV), simian retrovirus (SRV), simian T-cell leukemia virus (STLV), and simian foamy virus (SFV). Following quarantine, the macaques were fitted with collars and chair trained so that blood specimens could be withdrawn without anesthesia, which avoided interruption of food intake. A telemetry monitoring device (model T30F; Integrated Telemetry Services) was placed in an intramuscular pocket in the left abdominal wall of each animal; electrocardiographic leads were placed on the lateral left and right chest wall, an intrapleural pressure transducer was placed in the fifth intercostal space in the left part of the chest, and a temperature probe in a battery pack was placed in the lower abdominal musculature. The animals were moved into an animal biosafety level 3 laboratory at least 1 week before infection by the aerosol route for acclimatization and collection of baseline physiological measurements. The protocol and all amendments were reviewed and approved by the LRRI Institutional Animal Care and Use Committee.

Aerosol exposure. Macaques were exposed to *Y. pestis* strain CO92 via head-only inhalation of a target dose of 100 ± 50 ED_{50}. One aerosol ED_{50} in the cynomolgus macaque from Indonesia has been calculated to be 66 CFU (21). The term "ED_{50}" is used instead of 50% lethal dose (LD_{50}) because animals were euthanized prior to natural death in order to reduce suffering. Fasted animals were anesthetized with 4 mg/kg Telazol approximately 15 min prior to aerosol exposure. Each animal was placed on its back in a plethysmography box, with its head inserted through the dental dam head port into a head-only exposure apparatus in a class 3 biosafety cabinet as previously described (21). The bacteria were nebulized using a Collison nebulizer (MRE-3 jet; BGI, Inc.,

* Corresponding author. Mailing address: Lovelace Respiratory Research Institute, 2425 Ridgecrest Dr., Albuquerque, NM 87108. Phone: (505) 348-9614. Fax: (505) 348-8567. E-mail: fkoster@LRRI.org.

▽ Published ahead of print on 12 April 2010.

Waltham, MA) and delivered to the anesthetized monkey, which was allowed to breathe freely. Real-time plethysmography (Buxco) targeted an inhaled volume of 5 liters, and the actual exposure times ranged from 10 to 15 min. Aerosolized bacteria in the head exposure box were sampled using an all-glass impinger (AGI-4; Ace Glass, Inc., Vineland, NJ), and concentrations were confirmed by the quantitative bacterial culture method. The purity of each aerosolized sample was assessed by using colony morphology and growth on Congo red-containing media. The target particle size mass distribution (between 1 and 3 μm) was determined using a TSI aerosol particle sizer (model 3321; TSI, Inc., Shoreview, MN), which measured delivered aerosol particles whose sizes ranged from 0.5 to 20 μm (4). The pathogen dose was calculated using the following formula: dose = $C \times V$, where C is the concentration of viable pathogen in the exposure atmosphere and V is the total volume inhaled based on Buxco plethysmography and exposure time.

Preparation of bacteria for inhalation. Separate bacterial suspensions were prepared for each animal. Briefly, a working stock cryovial was removed from frozen storage, thawed, and used to inoculate five slants containing tryptose blood agar base with yeast extract (TBAB), which were incubated at 28°C ± 2°C for 72 h. Following incubation and verification of the purity, 2 ml of sterile 1% peptone was added to each slant. The bacterial growth was harvested using sterile, cotton-tipped wooden swabs and pooled (total volume, 10 ml). Each pooled suspension was centrifuged at 4,100 rpm and 5 to 6°C for 20 min. After disposal of the supernatant, the bacterial pellet was resuspended in 4 ml of 1% peptone and mixed thoroughly. Following standard 10-fold microbial dilution, a 100-fold dilution of the suspension was prepared and analyzed at a wavelength of 600 nm using a spectrophotometer. The resulting optical density data were compared to the working stock standard growth curve and used to estimate the titer. This starting concentration was used to calculate the dilution scheme required to obtain the target generator suspension concentrations. The generator suspensions were prepared based on a target inhaled volume of 3.5 liters. Challenge material was prepared in 10 ml (final volume) of sterile brain heart infusion broth (BHIB). Prior to delivery to the aerosol laboratory, 0.5 ml was removed for prebioaerosol analysis. Following removal of this aliquot, bacterial suspensions were weighed in order to establish a baseline for postbioaerosol volume calculations.

Clinical observations. Beginning on the first day of exposure, cage-side observation was performed on study monkeys twice a day (at least 4 h apart), and the characteristics examined included mortality, activity, nasal discharge, sneezing, coughing, ocular discharge, inappetance or anorexia, diarrhea, neurologic signs, and other abnormalities.

Telemetry. Vital signs and electrocardiogram (ECG) data were recorded continuously by implanted T30F telemetry devices (Integrated Telemetry Systems, Chicago, IL). Data were acquired every 0.01 s and were displayed as hour-average temperatures, respiratory rates, and heart rates. The temperature was recorded in the battery pack implanted intramuscularly in the abdominal wall. The respiratory rate was detected either by using changes in intrapleural pressure (T30F). The heart rate was recorded by using subcutaneous limb leads counting the number of R waves per minute. The respiratory and heart rates were calculated by the VR^2 software (D.I.S.S., Chicago, IL). ECG wave forms were recorded as raw data for real-time and subsequent review. A baseline temperature, a baseline respiratory rate, and a baseline heart rate were determined for each animal during the 4 days prior to aerosol challenge, and baseline hourly averages were used to calculate deviations from the normal diurnal variation. Each animal and its continuously recorded telemetry data were inspected in real time every 4 to 6 h after the first sign of illness in order to make a timely decision about euthanasia to reduce suffering. An animal was euthanized due to the appearance of moribund disease based on the development of at least two of the following criteria: body temperature less than 33°C, abnormal repolarization waveforms in an electrocardiogram consistent with ischemia or acute heart failure, deep labored breathing, seizures, too weak to climb onto a perch, and unresponsive to stimulation along with refusal to eat offered food.

Quantitative bacteriology. Venous blood (target volume, 1 ml) was withdrawn from the femoral vein and transferred to a tube containing EDTA. Anticoagulated blood was aliquoted for dilution and plating for quantitative bacteriology (CFU). The bacterial load was calculated by plating three dilutions of homogenized tissue or whole blood onto tryptic soy agar (TSA). The limit of detection was 200 CFU/ml blood. Following 72 h of incubation at 28°C, the purity was verified, and *Y. pestis* colonies were enumerated. Select colonies were placed into 1-ml cryovials containing sterile 1% peptone-15% glycerol and frozen at −80°C ± 10°C.

Bacterial DNA real-time qPCR. For purification of bacterial DNA, 100 μl of blood was immediately mixed with 900 μl of TRIZOL-LS buffer or 200 μl of homogenized tissue was immediately mixed with 800 μl of TRIZOL buffer, and each preparation was frozen until extraction was performed. A *Yersinia* 16S rRNA-specific molecular beacon quantitative PCR (qPCR) assay was developed for detection of *Y. pestis* DNA with the following primer and probe sequences (5′-3′): CACACTGGGCTACACCTGAA (sense primer), TGACAAAGTGGT TGCTGAGG (antisense primer), and CGCGATCCCAAGTTGTCCCCTGTG ACTGATCGCG (molecular beacon probe). The *Yersinia* 16S rRNA molecular beacon was labeled with 6-carboxyfluorescein (FAM) and quenched with 4-dimethylaminophenylazobenzoic acid (DABCYL). A second probe unique to the macaque glyceraldehyde-3-phosphate dehydrogenase (GAPDH) was used as an internal extraction and positive amplification control. The primer and probe sequences are as follows: CACACTGGGCTACACCTGAA (sense primer), TG ACAAAGTGGTTGCTGAGG (antisense primer), and CGCGATAGGGGTT GAGTTTAATACGCATCGCG (molecular beacon probe). The Macaca GAPDH molecular beacon was labeled with 6-carboxy-hexachlorofluorescein and quenched with DABCYL. The qPCR mixture (final volume, 50 μl) contained 2.0 μl of the extracted DNA, 1.0 μl of each primer (10 μM), 2.0 μl of each molecular beacon (5.0 μM), 25 μl of Brilliant II QPCR master mixture, and PCR-grade water. The qPCR assay was performed as a two-color multiplex reaction by using a Stratagene Mx3005P QPCR system. The thermal cycling parameters were one cycle of 10 min at 95°C, followed by 45 cycles of 30 s at 95°C, 30 s at 50°C, and 30 s at 72°C. Fluorescence (FAM and HEX) was measured at the annealing temperature. The lower limit of detection of the genus *Yersinia* 16S rRNA probe was 4 genome equivalents or 4 CFU of *Y. pestis* (data not shown; D. Perlin, unpublished data).

Serum and tissue chemokines and cytokines. Cytokine and chemokine contents were determined with Luminex bead assays using human antibody reagents (Biosource, Inc.) previously validated for specificity and sensitivity for macaque serum proteins. Serum from each macaque was analyzed prior to exposure, at necropsy, and at 48 h postexposure (p.e.) for three macaques that were expected to be necropsied at 96 h p.e.; for one of these three animals there was also a bronchoalveolar lavage specimen obtained at 48 h p.e. that was suitable for analysis. Two lung samples from each of the 12 necropsies, which weighed approximately 200 to 300 μg (wet weight), were homogenized in phosphate-buffered saline (PBS) and frozen at −80°C until they were analyzed. A total of 14 proteins, including 9 cytokines and 5 chemokines, were analyzed for 52 specimens from the 12 animals; thus, a total of 728 results were obtained in this analysis. The chemokines analyzed included RANTES, MIP-1α, MIP-1β, monocyte chemoattractant protein 1 (MCP-1), and IL-8. The cytokines analyzed included interleukin-1β (IL-1β), IL-2, IL-4, IL-6, IL-10, IL-12p40, gamma interferon (IFN-γ), granulocyte-macrophage colony-stimulating factor (GM-CSF), and tumor necrosis factor alpha (TNF-α). The assay for IL-1β and IL-6 has been validated previously (12), and the remainder of the assays were validated by the manufacturer.

Necropsy. When moribund euthanasia criteria were met or when a timed necropsy was performed, the animal was given 10 mg ketamine/kg of body weight intramuscularly and 2% isoflurane with a mask until deep anesthesia was obtained, and this was followed by exsanguination by cardiac puncture or, in some cases, by intravenous euthasol (pentobarbital sodium [86.7 mg/kg] plus phentoin [11.1 mg/kg]). Each necropsy was performed immediately after euthanasia, and the tissues used for bacteriologic and cytokine assays were collected and weighed. Lung lobes were gently inflated with neutral buffered formalin to obtain an approximately normal volume prior to immersion fixation. A lung sample was designated a "lung lesion" sample when it was collected from a discolored region that was also firm in order to avoid areas of discoloration due to euthanasia artifacts. A lung sample was designated a "lung nonlesion" sample when it was collected from an area without discoloration or firmness that appeared to be normal. Lung samples used for histopathology were taken from areas immediately adjacent to areas from which samples used for bacteriology and cytokine analysis were taken to permit parallel analyses to be performed. Lungs from animals necropsied at 24 h and 48 h after aerosol exposure had no apparent lesions, and the two samples from each lung used for parallel analyses were taken randomly from the caudal lobes. Sections of lungs, livers, spleens, tracheobronchial lymph nodes, and brains were processed routinely, embedded in paraffin, sectioned (thickness, 4 to 6 μm), mounted on standard glass slides, and stained with hematoxylin and eosin (H&E) for light microscopic examination. Lesions were graded subjectively by a single pathologist on a scale from 1 to 4 (grade 1, minimal; grade 2, mild; grade 3, moderate; grade 4, marked).

Statistics. Differences in values for telemetered vital signs compared with baseline values were tested by two-way analysis of variance (ANOVA) with repeated measures using Bonferroni posttests. Differences in cytokine and chemokine levels in serum and tissue between necropsy groups were tested by one-way ANOVA using Bonferroni posttests.

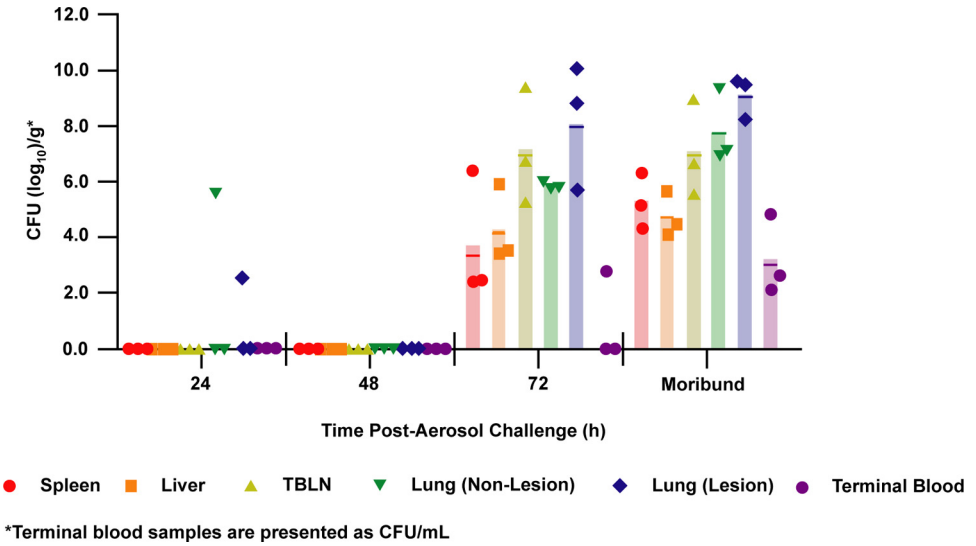

FIG. 1. Bacterial culture of blood and tissue collected at scheduled necropsies (24, 48, and 72 h postchallenge) and after euthanasia of moribund macaques following aerosol exposure to *Y. pestis*. The results are expressed as $\log_{10}$ CFU per gram of tissue or per milliliter of whole blood. Samples from three animals were analyzed for each time point for scheduled necropsies (24 h, 48 h, and 72 h), and three moribund animals were necropsied at 70 h, 92 h, and 94 h p.e. The bars indicate means for the three samples; the value for each sample was the mean for three replicate cultures (symbols). TBLN, tracheobronchial lymph nodes.

RESULTS

Four groups, each containing three telemetered adult macaques, were challenged by the aerosol route with *Y. pestis* using doses of 141 ± 32 ED_{50} (group mean ± standard deviation). Animals were scheduled to be euthanized and necropsied 24, 48, 72, and 96 h postexposure (p.e.); the three animals in the 96-h group were moribund and were actually necropsied at 70 h, 92 h, and 94 h p.e.

Quantitation of bacteria. Small numbers of *Y. pestis* cells were cultured for two of six lung samples at 24 h p.e., while all blood, lymph node, liver, and spleen cultures were negative at 24 h p.e. (Fig. 1). The organisms in the positive lung cultures with low levels of bacteria may have represented residual bacteria from the inhalation exposure or may have been small foci of persistent bacteria that later expanded to pneumonic regions. All cultures were negative at 48 h p.e. Bacteremia was detected in one of three macaques scheduled to be necropsied at 72 h p.e. and was also detected in the three animals which were moribund at 70 h, 92 h, and 94 h p.e. In contrast, lungs and tracheobronchial lymph nodes had substantial bacterial loads at 70 to 72 h p.e., and there were higher numbers of *Y. pestis* cells in visibly consolidated lesions than in normal-appearing lung tissue, a difference that was not evident by 96 h p.e.

The lower limit of detection when 100 μl of blood was plated was 200 CFU/ml blood. To detect lower levels of bacteremia, we used a real-time PCR molecular beacon probe specific for the *Yersinia* 16S rRNA subunit. A second probe for macaque GAPDH provided an internal extraction control and positive amplification control. The GAPDH cycle threshold (C_T) values were a measure of the extraction efficiency and ranged from 25 to 37. C_T values for GAPDH of >35 indicated inadequate nucleic acid recovery and were obtained for only 3 of 36 samples. The lower limit of detection of the 16S rRNA probe was 4 genome equivalents (Fig. 2A), which was equivalent to 4 CFU of *Y. pestis*. At 24 h p.e. all blood samples were negative and one of two culture-positive lung samples was positive as determined by reverse transcription-PCR (RT-PCR). At 48 h p.e. all samples were negative as determined by culture and RT-PCR. At 72 h p.e. all 18 blood and tissue samples were positive as determined by RT-PCR, including two blood samples that were negative when the culture method was used. All 18 samples from moribund animals were positive as determined by both assays. A comparison of 20 tissue samples that were positive with both assays (Fig. 2B) revealed that there was good quantitative correlation among samples from moribund animals ($r = 0.87$, $P < 0.01$) but not among samples collected at 72 h p.e. ($r = 0.2$, not significant).

Disease progression and telemetered physiology. Telemetered data displayed as hour averages for heart rate, respiratory rate, and temperature superimposed on the preexposure diurnal variation are shown in Fig. 3 for two macaques observed until they were moribund 96 h after aerosol exposure; data for the six macaques that survived until at least 70 h p.e. are not shown (complete telemetry data is available at http://dspace.lrri.org:8080/xmlui/handle/123456789/871). The onset of an abnormal body temperature, as defined by a statistically significant departure from the baseline diurnal value, was seen at 60 h p.e. (Fig. 3) for both animals, although the temperature did not exceed 39°C until 68 h and 75 h p.e., respectively. Three of the four animals necropsied at 70 to 72 h p.e. had initial elevated temperatures at 55 to 60 h p.e., although none had a persistent temperature greater than 39°C. Six animals had tachypnea, and five of these six animals had tachycardia above the baseline value, including the animal in which the temperature was not elevated. The onset of tachycardia and tachypnea appeared to coincide with the onset of fever as defined by departure from the baseline value, but markedly

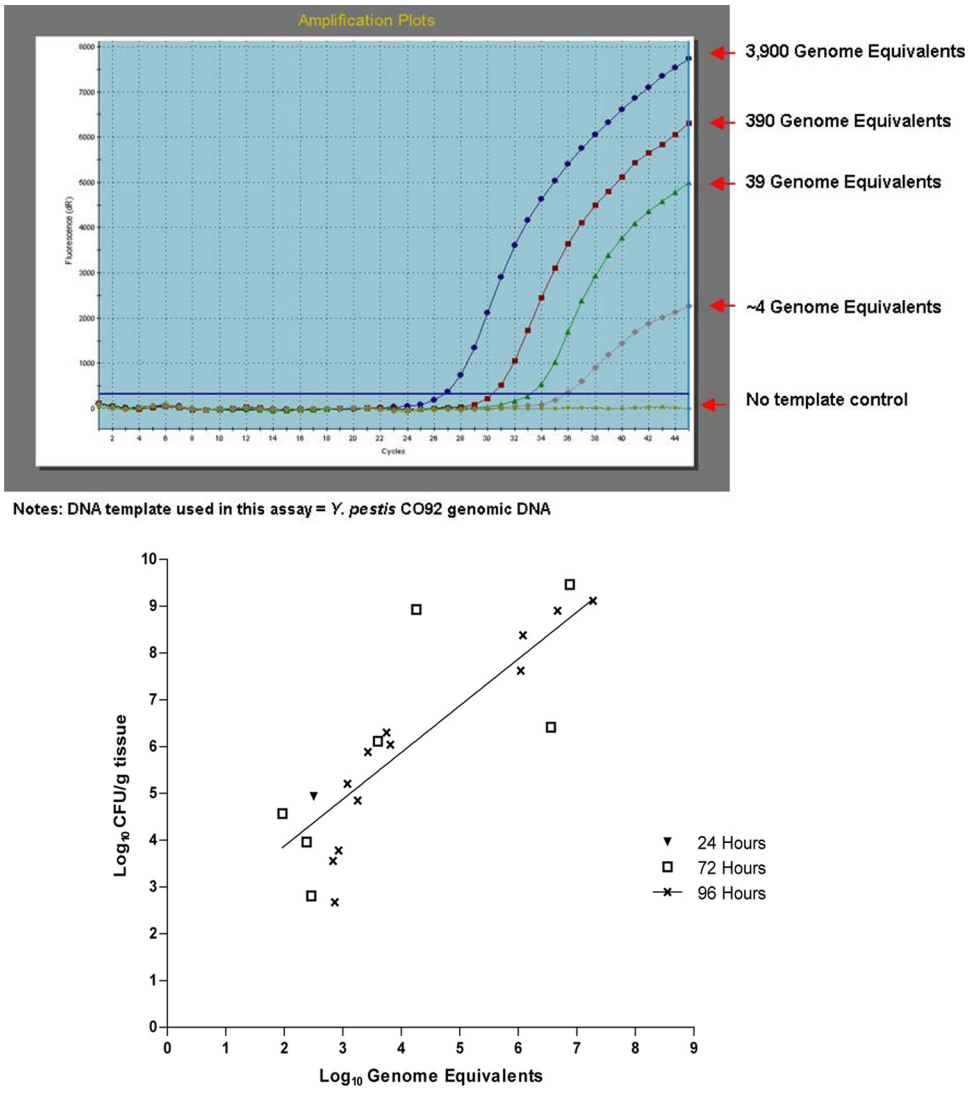

FIG. 2. (Top panel) Sensitivity of the real-time RT-PCR assay specific for *Y. pestis* rRNA. (Bottom panel) Correlation of quantitative results of bacterial culture and RT-PCR analyses for tissue samples positive with both assays. The results for samples that were determined to be positive by only one assay are described in the text. The line was derived from the regression equation relating numbers of genome equivalents and CFU for each tissue sample collected from moribund animals.

elevated heart and breathing rates were not seen until after 72 h p.e. By 72 h p.e. most animals showed markedly depressed activity and were withdrawn and immobile at the back of their cages in a hunched posture. As they became moribund, these animals were hypothermic, had decreasing respiratory rates and pulses, and were no longer able to balance on their perches .

Cytokine and chemokine response. The levels of cytokines and chemokines were not elevated compared to preexposure levels or these proteins were not detected in serum or lung tissue at 24 h and 48 h p.e. (Fig. 4) (data not shown). Elevated levels of three cytokines and three chemokines were found in some lung tissue but not in serum at 72 h p.e. Few differences in the 48-h and 72-h levels were statistically significant, however, likely due to the small group size (three animals for each comparison). The levels of IL-1β were elevated in lung lesions ($P < 0.001$), and the levels of the chemokines CCL2 (MCP-1) and CCL3 (MIP-1α) were elevated in most lesion and nonlesion lung samples ($P < 0.01$). In moribund animals the tissue levels of cytokines and chemokines were not different from the levels in nonmoribund animals at 72 h p.e. When the other eight chemokines and cytokines that were measured were examined, either they were not detected in any serum or tissue sample or their levels were not elevated following infection (data not shown). One animal was clinically well and afebrile when it was necropsied at 72 h p.e. and had bacteremia with *Y. pestis* demonstrable only by RT-PCR. This animal had low but detectable levels of TNF-α and IL-6 in its lung tissue, and it was the only animal with an elevated IL-10 level in preexposure serum.

Pathology. The gross appearance of the lungs was characterized by multifocal areas of pneumonia along with enlarged tracheobronchial lymph nodes (Fig. 5). Consolidated regions with pneumonia were apparent and were palpably firm, mod-

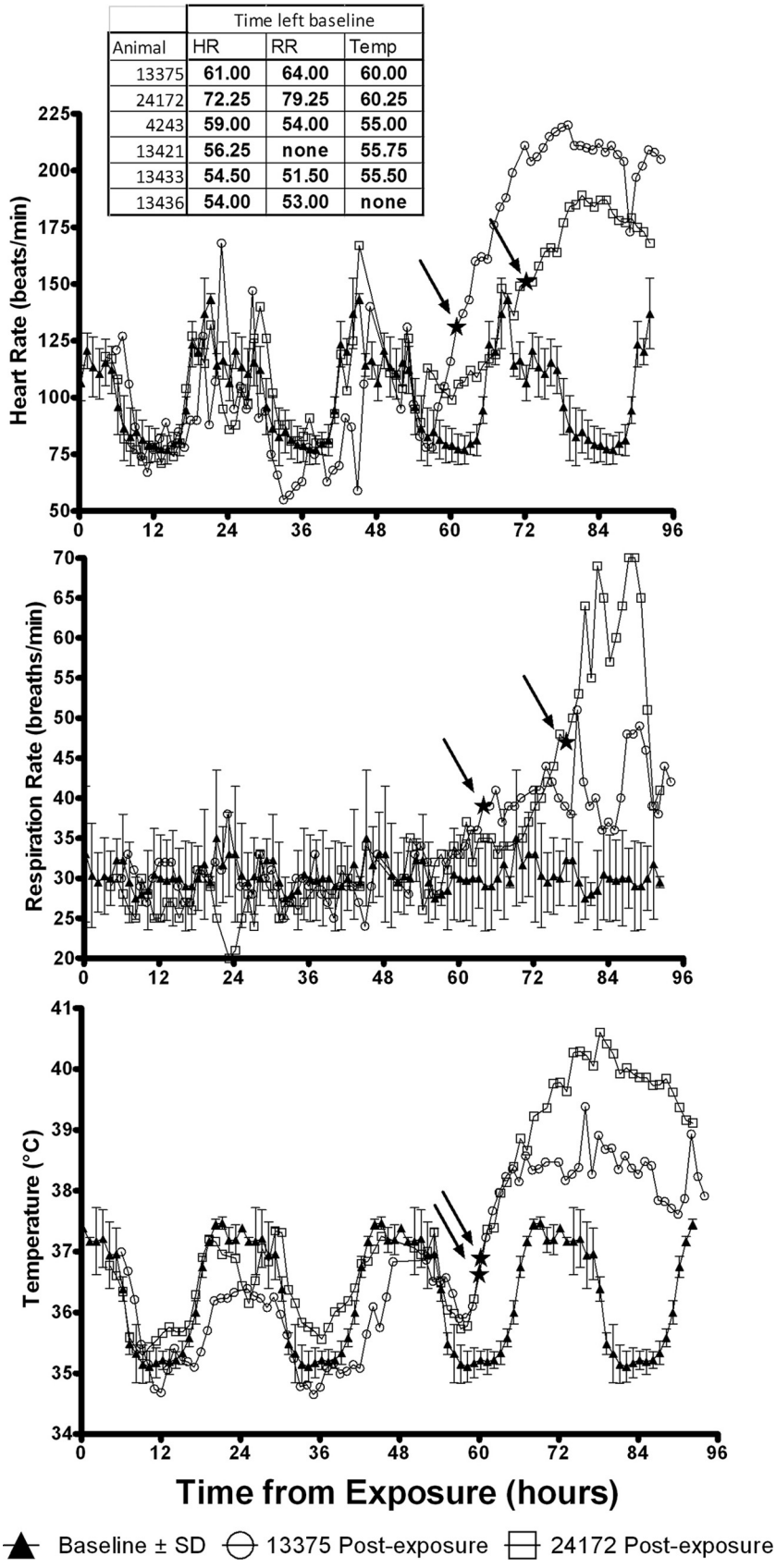

FIG. 3. Telemetery physiological data for two macaques that were moribund at 92 and 94 h p.e. The heart rates (HR) (top panel), respiratory rates (RR) (middle panel), and body temperatures (bottom panel) shown are 1-h averages for each animal. The baseline data are data for each animal averaged for each

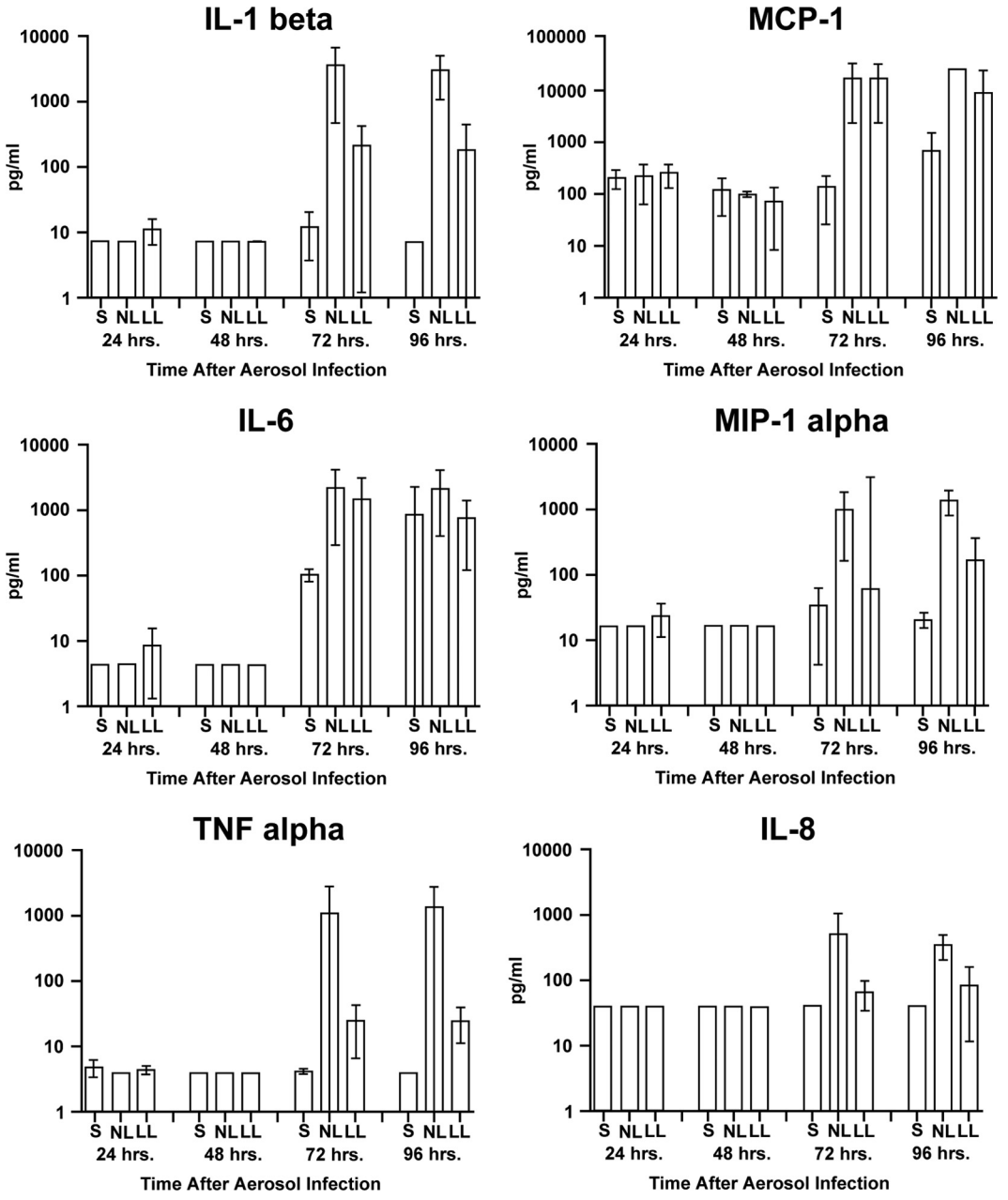

FIG. 4. Cytokine and chemokine levels (means and standard deviations) for three samples each for serum (S), lung tissue with lesions (LL), and normal-appearing lungs (NL) collected at scheduled necropsies at 24 h, 48 h, and 72 h p.e. Three animals in the 96-h group were moribund at necropsy at 70 h, 92 h, and 94 h p.e.

erately well-demarcated regions with different amounts of dark red discoloration and hemorrhage. At 24 h p.e., no lesions which could be attributed to *Y. pestis* infection were found. In the tissue samples examined histologically (Fig. 6E), there was no detectable pathology, although two positive bacteriologic cultures (Fig. 1) likely represented small early foci of pneumonia. At 48 h p.e., the results for only one of three lungs (from animal 13422) suggested that there was a possible early focus of infection, and there was alveolar thickening due to mononuclear cell infiltration (Fig. 6A), but no bacilli were seen.

hour of the day over 4 days of preexposure recording. The baseline data for animal 24172 are data for 24-h periods showing diurnal variation; the baseline data for animal 13375 are similar to the baseline data for animal 24172 and are not shown. Data were compared to each animal's baseline diurnal variation results by using two-way ANOVA with repeated measures and Bonferroni posttests. The times when the values begin to be significantly different from the animal's baseline values are indicated by filled stars; arrows indicate the locations of the filled stars for clarity.

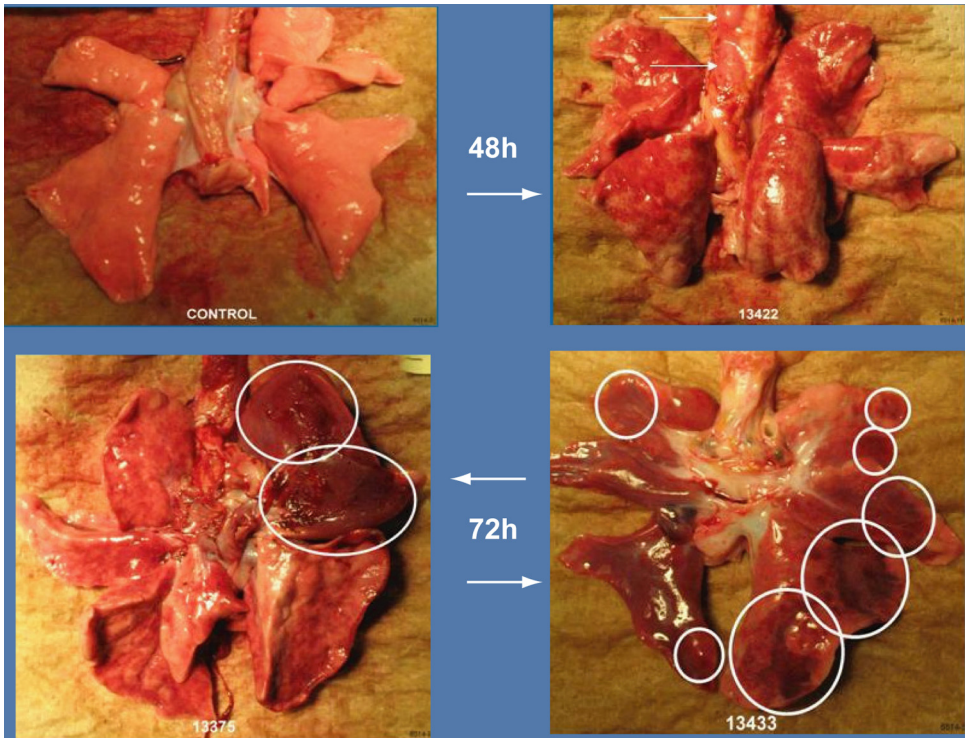

FIG. 5. Images of macaque lungs. (Upper left panel) Uninfected control. (Upper right panel) Lung 48 h after infection. The arrows indicate enlarged tracheobronchial lymph nodes, and the gray peripheral regions are due to an anesthesia artifact. (Lower panels) Lungs at 72 h p.e. Ellipses and circles indicate palpably firm nodules in lung parenchyma that were identified as lesion regions.

Occasional chronic inflammation was seen in the lungs of some animals (Fig. 6E), and it was likely attributable to chronic changes observed in the wild-caught macaques used.

Timed necropsies revealed the explosive progression of disease between 48 h p.e. and 72 h p.e. (Fig. 6B to E). By 72 h p.e. distinct focal lesions were consistent with fibrinosuppurative pneumonia and alveolar edema and were confirmed histologically (Fig. 6B). In contrast, in the nonlesion lung areas there was typically multifocal, mild septal, and/or alveolar infiltration with neutrophils and mononuclear cells (Fig. 6C). By 96 h p.e., however, identification of a "nonlesion" sample often was difficult, and such samples often exhibited similar, although less extensive, pneumonia histologically (Fig. 6D and E). The culture experiments also demonstrated that there was wide distribution of bacteria by 96 h p.e., likely due to the bacteremia distributing infection throughout all areas of the lungs.

The areas where there was mixed alveolar inflammation and pneumonia contained primarily septal and alveolar neutrophils and macrophages. Areas of necrosis were present in severe foci of pneumonia, and extension to surrounding compartments (airways, vasculature) was observed. The areas of pneumonia in these animals were typically deep in the pulmonary parenchyma and often were not associated with airways, which is common in many classic, naturally acquired inhalation pneumonias (e.g., bronchopneumonia). This may have been a result of secondary hematogenous spread to or within the lungs after initial phagocytosis by macrophages, combined with the initial insult, which often occurred deep in the lung due to the well-dispersed aerosol administered. Areas of alveolar edema were indicated by eosinophilic background staining in alveolar air spaces. Basophilic, short, rod-shaped cells typical of *Y. pestis* were visible both extra- and intracellularly in most cases when there was substantial pneumonia (the characteristic bipolar staining or "safety pin" appearance is often not prominent with tissue section staining with H&E). Where these bacteria were most abundant, they were typically scattered throughout the alveoli in the edema fluid. Fibrinosuppurative pleuritis was seen occasionally with severe pneumonia and was likely an extension of this process.

The liver and spleen were grossly unremarkable in this study and were not examined histologically. Related studies have demonstrated that the livers of affected cynomolgus macaques are typically relatively unremarkable and are characterized principally by mild to moderate sinusoidal leukocytosis (an increase in the number of white blood cells in the hepatic sinusoids). In most cases the leukocytes are primarily neutrophils, and there are fewer monocytes and lymphocytes. The splenic histopathology is essentially similar to the histopathology of the liver, and a similar sinusoidal leukocytosis is the principal change. Scattered bacteria to moderate numbers of bacteria are occasionally evident in monocytes/macrophages in the spleen. The leukocytosis in the liver and spleen probably reflects to some extent a systemic increase in the number of circulating white blood cells in response to disease. Similarly, the tracheobronchial lymph nodes (adjacent to the tracheal bifurcation or carina) usually exhibit sinusoidal leukocytosis characterized principally by macrophages. Often bacteria are relatively frequent in the cytoplasm of monocytes/macrophages

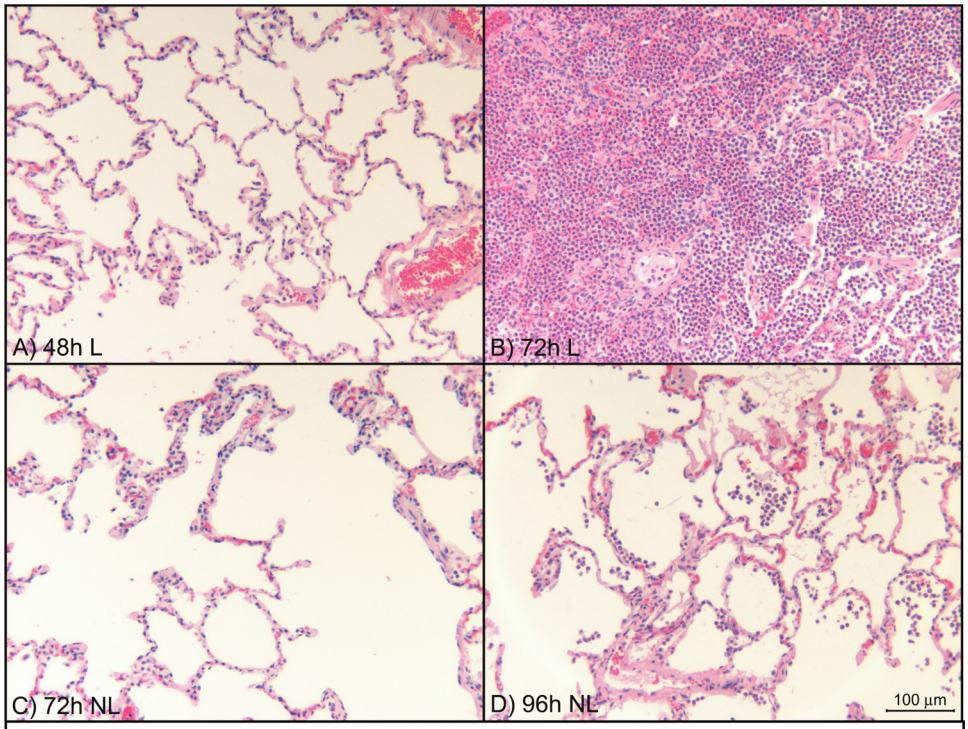

E Necropsy Group	24h PE			48h PE			72h PE			96h PE		
Animal number	*13461*	*13463*	*20192*	*13422*	*20182*	*24155*	*4243*	*13421*	*13436*	*13375*	*13433*	*24172*
LUNG												
Inflammation alveolar	0	0	0	0	0	0	4	4	1	4	3	4
Edema, alveolar	0	0	0	0	0	0	4	4	0	4	3	4
Bacteria	0	0	0	0	0	0	3	3	0	0	0	3
Pleuritis	0	0	0	0	0	0	0	3	0	0	0	0
Inflammation mono	0	0	0	2	0	0	0	0	1	0	0	0
alveolar macrophages	0	0	0	1	0	0	0	0	0	0	0	0

FIG. 6. Histopathology in lung regions with gross abnormality (lesions [L]) and without gross abnormality (no lesions [NL]). (A) Normal-appearing lung with focal thickened alveolar septa (grade 1) at 48 h p.e. (B) Firm nodule (lesion) with hemorrhage and severe alveolitis (grade 4) at 72 h p.e. (C) Normal-appearing lung (no lesions) adjacent to tissue shown in panel B at 72 h p.e, with diffuse thickened alveolar septa (grade 2). (D) Normal-appearing lung (no lesions) at 96 h p.e., with congestion and alveolitis (grade 3). (E) Histopathological scores for lung tissues from 12 macaques. The "moribund" group included three animals that were euthanized because they were moribund at 70 h, 92 h, and 94 h p.e. "Inflammation alveolar" indicates predominantly polymorphonuclear leukocyte infiltration, while "inflammation mono" indicates mononuclear leukocyte infiltrate without neutrophils.

in these draining lymph nodes. None of these tissues have been observed to have focal inflammatory nodules or necrosis grossly or in areas examined histologically.

DISCUSSION

The purpose of characterizing nonhuman primate models of inhalational plague is to improve preclinical evaluation of candidate vaccines and treatments (11). Primary pneumonic plague in the cynomolgus macaque mimics primary pneumonic plague in humans in many important respects (5, 9, 18, 22). In both humans and macaques the incubation period is short, and there is rapid progression to severe illness, fever, tachypnea, tachycardia, bacteremia in most but not all cases, an absence of hepatosplenomegaly and lymphadenopathy, minimal transaminasemia, often marked blood leukocytosis, and extensive patchy multilobar pneumonia. Features of the human disease not shared by the cynomolgus macaque disease include coughing, hemoptysis, thrombocytopenia, and coagulopathy.

The primary findings of this natural history study indicate that severe primary pneumonic plague is characterized by two phases, an anti-inflammatory phase and a proinflammatory phase, similar to the phases described for inbred and outbred mouse strains (3, 14). In mice the early phase, characterized by low concentrations of nonviable bacteria in lung macrophages and a lack of a pulmonary cytokine and chemokine response, was followed by explosive growth of *Y. pestis* in the lung and dissemination to the spleen by 36 h. The apparent 24- to 48-h lag phase in the lung may be related to genetic switches that the *Y. pestis* genome must undergo in the 37°C mammalian environment (14, 15).

Y. pestis expresses a number of virulence determinants, particularly the Yop virulons (6, 17). Yop proteins mediate antiphagocytic effects by dephosphorylating key focal adhesion proteins, inactivating GTPases that control cytoskeleton dynamics, preventing activation of the master inflammation regulator NFκB, and inducing macrophage and dendritic cell apoptosis (2). The effects of this initial paralysis of host phagocytosis mechanisms may have been seen in our macaques, as

suggested by the lack of a cytokine or chemokine response in lung tissue and the lack of neutrophil recruitment at 48 h p.e.

Substantial variability in the host response to aerosolized *Y. pestis* was seen in wild-captured macaques. The animals were exposed to approximately 4,000 to 9,000 viable aerosolized bacteria in their breathing zone. This inhaled dose represents an estimated LD_{95}, not an LD_{100}, as we have observed that macaques occasionally survive supralethal doses (7). The gross pathology typically included less than 10 distinct inflammatory foci, separated by large areas of normal tissue, in each lung at 72 h p.e. Only about 5 to 10% of 1- to 3-μm inhaled particles are deposited in the alveolar region of the lungs of NHP, and there is greater deposition in the upper airways, including the nasopharynx and tracheal regions (4). If as few as 10 CFU of bacteria initiate disease in the alveoli, a large percentage of bacteria that reach the alveoli are killed by innate defenses. In the study that calculated the ED_{50} for cynomolgus macaques (21), an animal exposed to as few as 35 *Y. pestis* bacteria survived, while another animal exposed to 270 bacilli died. In this study one macaque (animal 13436) with an elevated serum IL-10 level before exposure exhibited mild clinical disease and did not have an elevated temperature; in addition, *Y. pestis* was detected in the blood only by qPCR, and there were low levels of cytokines in the lung tissue at necropsy at 72 h p.e. These observations suggest that in cynomolgus macaques there are individual variations in critical innate lung defenses which may modulate survival.

An important milestone in the progression of disease is the onset of bacteremia. For one animal a blood culture was negative at 72 h p.e. in spite of onset of fever at 60 h p.e. The sensitivity of bacteremia detection method is limited by the low plate inoculum volume (100 μl, corresponding to a lower limit of detection of 200 CFU per ml of blood). The highly sensitive *Yersinia* rRNA-specific quantitative real-time PCR (Fig. 2A) detected rRNA in all blood and tissue at 72 h p.e. Even qPCR is limited by the sample isolation procedure, since the 48-h macaque blood GAPDH C_T values were at least three times less than the values for the other time points, indicating that there was at least 10 times less DNA in the samples. Although our sample size was small, the qPCR assay that detects rRNA may be the preferred method when the onset of bacteremia must be detected with sensitivity.

Fever is the first evidence of systemic disease and is an important milestone that is useful for initiating postexposure treatment. In the six macaques observed for more than 48 h p.e., the onset of significant temperature elevation occurred consistently between 55 h and 60 h p.e. The onset of fever may have preceded the onset of bacteremia, as bacteremia was detected only by qPCR and not by the culture method in two of three febrile macaques at 72 h p.e. Several macaques did not develop a body temperature greater than 39°C in the current study. Measurements of body temperature with a rectal thermometer, like those obtained in a previous study (21), are subject to bias introduced by anesthesia and often differ from simultaneous measurements obtained by using implanted chips (19). Intermittent measurement may miss the onset of fever, delaying the onset of treatment. Here, continuous telemetry identified the onset of fever when there was an abrupt departure from the normal diurnal pattern (Fig. 3), and an absolute temperature of more than 39°C was not always documented.

The heart rate and respiratory rate appeared to increase to values above the diurnal rhythm limits at the same time that the temperature increased (Fig. 3), but such increases were often not apparent when the data were inspected in real time due to minute-to-minute variations. Estimation of the respiratory rate in nonhuman primates by observation alone is difficult. Although a recent study found that there was no respiratory distress (21), we observed respiratory distress with labored breathing in most animals after 60 h p.e., and tachypnea in all animals was confirmed by telemetry. These observations agree with previous reports of respiratory distress (1, 10). Tachypnea in our animals was a sign of successful compensation for modest hypoxemia, as in other studies we have found no evidence of respiratory acidosis and failure (R. C. Layton and F. Koster, unpublished observations). Telemetric measurements also allowed us to identify more precise indicators of impending death and thus allowed us to prevent unnecessary suffering while avoiding the error of euthanizing an animal which may have survived in spite of illness. Repolarization abnormalities in the ECG, either ST segment depression or T wave inversion, were the most consistent indicators of irreversible disease and have never been seen in survivors (R. C. Layton and F. Koster, unpublished data).

Observations in this study confirmed the similar clinical and histopathological features of pneumonic plague in nonhuman primate and human hosts and identified important parallels with the murine model of pneumonic plague. In future studies we will compare the appearance of secondary endpoints of efficacy, including bacteremia and telemetered vital signs, in immunized and nonimmunized cynomolgus macaques.

ACKNOWLEDGMENTS

This work was supported by grant U54 AI057156 from the Regional Centers of Excellence in Emerging Infections and Biodefense.

We thank Lorena Diehl for flow cytometry, veterinarians for telemetry device insertion, the microbiology staff, and the Animal Technical Pool and necropsy personnel of the ABSL3 at LRRI for expert animal care.

REFERENCES

1. **Adamovicz, J. J., and P. L. Worsham.** 2006. Plague, p. 107–135. *In* J. Swearengen (ed.), Biodefense research methodology and animal models. Taylor & Francis, Boca Raton, FL.
2. **Bosio, C. M., A. W. Goodyear, and S. W. Dow.** 2005. Early interaction of *Yersinia pestis* with APCs in the lung. J. Immunol. **175:**6750–6756.
3. **Bubeck, S. S., A. M. Cantwell, and P. H. Dube.** 2007. Delayed inflammatory response to primary pneumonic plague occurs in both outbred and inbred mice. Infect. Immun. **75:**697–705.
4. **Cheng, Y. S., H. Irshad, P. Kuehl, T. D. Holmes, R. Sherwood, and C. H. Hobbs.** 2008. Lung deposition of droplet aerosols in monkeys. Inhal. Toxicol. **20:**1029–1036.
5. **Cohen, R. J., and J. L. Stockard.** 1967. Pneumonic plague in an untreated plague-vaccinated individual. JAMA **202:**365–366.
6. **Cornelis, G. R.** 2000. Molecular and cell biology aspects of plague. Proc. Natl. Acad. Sci. U. S. A. **97:**8778–8783.
7. **Cornelius, C. A., L. E. Quenee, K. A. Overheim, F. Koster, T. L. Brasel, D. Elli, N. A. Ciletti, and O. Schneewind.** 2008 Immunization with recombinant V10 protects cynomolgus macaques from lethal pneumonic plague. Infect Immun **76:**5588–5597.
8. **Davis, K. J., D. L. Fritz, L. M. Pitt, S. Welkos, P L. Worsham, and A. Friedlander.** 1996. Pathology of experimental pneumonic plague produced by fraction-1-positive and fraction-1-negative *Yersinia pestis* in African green monkeys. Arch. Pathol. Lab. Med. **120:**156–162.
9. **Doll, J. M., P. S. Zeitz, P. Ettestad, A. L. Bucholtz, T. Davis, and K. L. Gage.** 1994. Cat-transmitted fatal pneumonic plague in a person who traveled from Colorado to Arizona. Am. J. Trop. Med. Hyg. **51:**109–114.
10. **Finegold, M. J., J. J. Petery, R. F. Berendt, and H. R. Adams.** 1968. Studies on the pathogenesis of plague. Blood coagulation and tissue responses of

Macaca mulatta following exposure to aerosols of Pasteurella pestis. Am. J. Pathol. **53:**99–114.
11. **Food and Drug Administration Center for Biologics Evaluation and Research and Department of Health and Human Services.** 2004. Proceedings of the Public Workshop on Animal Models and Correlates of Protection for Plague Vaccines Workshop. Department of Health and Human Services, Washington, DC.
12. **Giavedoni, L. D.** 2005. Simultaneous detection of multiple cytokines and chemokines from non-human primates using Luminex technology. J. Immunolog Methods **301:**89–101.
13. **Inglesby, T. V., D. T. Dennis, D. A. Henderson, J. G. Bartlett, M. S. Ascher, E. Eitzen, A. D. Fine, A. M. Friedlander, J. Hauer, J. F. Koerner, M. Layton, J. McDade, M. T. Osterholm, T. O'Toole, G. Parker, T. M. Perl, P. K. Russell, M. Schoch-Spana, and K. Tonat.** 2000. Plague as a biological weapon: medical and public health management. Working Group on Civilian Biodefense. JAMA **283:**2281–2290.
14. **Lathem, W. W., S. D. Crosby, V. L. Miller, and W. E. Goldman.** 2005. Progression of primary pneumonic plague: a mouse model of infection, pathology, and bacterial transcriptional activity. Proc. Natl. Acad. Sci. U. S. A. **102:**17786–17791.
15. **Lawson, J. N., C. R. Lyons, and S. A. Johnston.** 2006. Expression profiling of *Yersinia pestis* during mouse pulmonary infection. DNA Cell Biol. **25:**608–616.
16. **Meyer, K. F., G. Smith, L. Foster, J. D. J. Marshall, and D. C. Cavanaugh.** 1974. Plague immunization. IV. Clinical reactions and serologic response to inoculations of haffkine and freeze-dried plague vaccine. J. Infect. Dis. **129:** S30–S36.
17. **Perry, R. D., and J. D. Fetherston.** 1997. *Yersinia pestis*—etiologic agent of plague. Clin. Microbiol. Rev. **10:**35–66.
18. **Ratsitorahina, M., S. Chanteau, L. Rahalison, L. Ratsifasoamanana, and P. Boisier.** 2000. Epidemiological and diagnostic aspects of the outbreak of pneumonic plague in Madagascar. Lancet **355:**111–113.
19. **Sikoski, P., M. L. Banks, R. Gould, R. W. Young, J. M. Wallace, and M. A. Nader.** 2007. Comparison of rectal and infrared thermometry for obtaining body temperature in cynomolgus macaques (*Macaca fascicularis*). J. Med. Primatol. **36:**381–384.
20. **Smith, P. N.** 1959. Pneumonic plague in mice: gross and histopathology in untreated and passively immunized animals. J. Infect. Dis. **104:**78–84.
21. **Van Andel, R., R. Sherwood, C. Gennings, C. R. Lyons, J. Hutt, A. Gigliotti, and E. Barr.** 2008. Clinical and pathologic features of cynomolgus macaques (*Macaca fascicularis*) infected with aerosolized *Yersinia pestis*. Comp. Med. **58:**68–75.
22. **Werner, S. B., C. E. Weidmer, B. C. Nelson, G. S. Nygaard, R. M. Goethals, and J. D. Poland.** 1984. Primary plague pneumonia contracted from a domestic cat at South Lake Tahoe, California. JAMA **251:**929–931.

Editor: J. B. Bliska